

Thickness diffusivity in the Southern Ocean

Carsten Eden¹

Received 27 February 2006; revised 11 April 2006; accepted 19 April 2006; published 8 June 2006.

[1] Thickness diffusivity (κ) according to the Gent and McWilliams parameterisation which accounts for eddy-driven advection in the ocean, is estimated using output from an eddy-resolving model of the Southern Ocean. A physically meaningful definition of rotational eddy fluxes leads almost everywhere to positive κ . Zonally averaged near surface values of κ remain smaller than 200 m²/s poleward of the polar front, increases between 60–45°S to about 600 m²/s and peak between 45–35°S at almost 3000 m²/s. κ stays high in the upper 500 m but decreases with depth and is essentially zero below 2500 m. In addition to the thickness diffusion (κ) there is eddy-induced eastward (westward) advection of isopycnal thickness at the poleward (equatorward) flank of the ACC pointing toward strong anisotropic lateral mixing. **Citation:** Eden, C. (2006), Thickness diffusivity in the Southern Ocean, *Geophys. Res. Lett.*, 33, L11606, doi:10.1029/2006GL026157.

1. Introduction

[2] In the Southern Ocean, eddy-driven transports can be as large as mean transports. In particular the meridional, cross frontal transports are affected or even controlled by meso-scale eddy activity. In ocean models, such variability has to be adequately resolved or parameterised. The parameterisation by *Gent and McWilliams* [1990, hereinafter referred to as GM] is currently used to account for such eddy-driven transports, in which the so-called thickness diffusivity (κ) has to be specified. Only a rough order of magnitude is currently known for κ , but, in particular in the Southern Ocean, the choice of κ strongly affects meridional transports of mass and tracers [*England and Rahmstorf*, 1998] and is therefore of crucial importance to quantify the role of the Southern Ocean in the climate system.

[3] Currently, constant values of 1000 m²/s are typically chosen in ocean climate models, sometimes higher in the upper ocean and lower below the thermocline, but it is clear that the thickness diffusivity should also have spatial dependency [*Ferreira et al.*, 2005; *Eden et al.*, 2006]. Because of the sparseness of observations it appears difficult to estimate κ directly from available observations, although there have been some attempts in the Southern Ocean [*Phillips and Rintoul*, 2000]. On the other hand, several authors have tried to infer κ from eddy-resolving general circulation models [e.g., *Rix and Willebrand*, 1996]. However, these attempts have only been partly successful even in determining the overall gross magnitude of κ in the ocean. It has been suggested by *Bryan et al.* [1999] that part

of the difficulties estimating thickness diffusivities from data are related to the presence of rotational eddy fluxes, which do not effect the divergence of the total fluxes and thus the mean tracer budgets, but do effect the estimated κ .

[4] Using data from a realistic eddy-resolving model of the North Atlantic, *Eden et al.* [2006] choose a definition of rotational fluxes originally proposed by *Marshall and Shutts* [1981] and refined by *Medvedev and Greatbatch* [2004] to estimate κ . It was shown that results are indeed physically more plausible when rotational fluxes are taken into account. In all their estimates, *Eden et al.* [2006] show κ , diagnosed from the horizontal eddy flux of buoyancy down the horizontal gradient of mean density, and a new parameter (ν) related to a previously neglected component of the eddy flux along, rather than across, the mean density contours. The ν -related part of the flux accounts for non-isotropic lateral mixing and is not included in the original GM parameterisation.

[5] Here, a corresponding analysis is presented for the Southern Ocean. In section 2, a simulation of an eddy-resolving model of the Southern Ocean is briefly evaluated and compared with available observations. In section 3, estimated thickness diffusivities are discussed and in section 4 results are summarised and discussed.

2. Model Description and Evaluation

[6] The model is based on a rewritten version of MOM2 [*Pacanowski*, 1995] and similar to the one used by *Eden et al.* [2006] except for the following differences: The horizontal resolution of the model is 1/10° with 42 vertical levels ranging from 10m at the surface to 250m at depth. The model domain covers the latitudinal belt between 78°S to 30°S with open boundaries at 30°S with prescribed barotropic inflow and a standard second order centered differences advection scheme is used. The model is integrated in a spin-up phase of 10 years followed by a 5-year analysis period. Biharmonic diffusion and friction are used with diffusivity and viscosity of 0.8×10^{10} m⁴/s and 2×10^{10} m⁴/s respectively.

[7] Figure 1a shows the 5-year mean barotropic stream function in the model. Most prominent is the eastward transport associated with the Antarctic Circumpolar Current (ACC). The mean ACC transport in the Drake Passage between the southern tip of South America and the Antarctic Peninsula is ca. 122 Sv (1 Sv = 10⁶ m³/s); the transport of the ACC itself is about 130 Sv, but there is a weak recirculation of a ca. 8 Sv near the Antarctic Peninsula. The transport of the Weddell (Ross) gyre is about 70–80 Sv (60 Sv), which is close to observational estimates [e.g., *Rintoul et al.*, 2001].

[8] Figure 1b shows the near surface mean kinetic energy (MKE = $\frac{\bar{u}^2 + \bar{v}^2}{2}$). The surface flow of the ACC around Antarctica breaks up into several branches which are related

¹Leibniz Institute of Marine Sciences at University of Kiel (IFM-GEOMAR), Kiel, Germany.

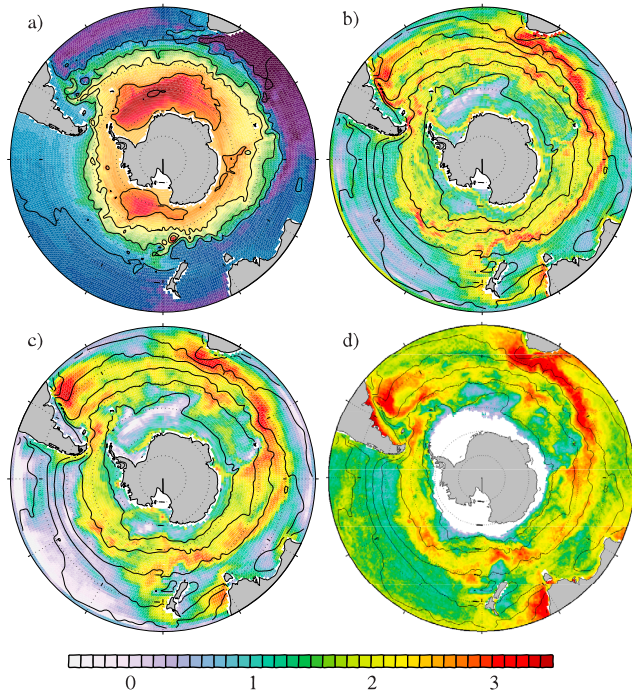


Figure 1. (a) 5-year mean barotropic stream function in Sv (contour interval 50 Sv). (b) Logarithm of MKE at 15 m depth in $\log(\text{MKE}/[\text{cm}^2/\text{s}^2])$. (c) Same as Figure 1b but for EKE. (d) Same as Figure 1c but estimated from altimeter data from the years 2003–2005. The colour bar refers to Figures 1b–1d in which also mean (model) density contours are shown ($\sigma_\theta = 27.37, 26.96, 26.56, 26.15, 25.75$ and 25.34 kg/m^3). The altimeter products have been produced by SSALTO/DUACS and are distributed by AVISO.

to the polar fronts. The MKE is closely related to the eddy kinetic energy ($\text{EKE} = \frac{u'^2 + v'^2}{2}$) (Figure 1c). Amplitudes and large scale distribution are very similar for MKE and EKE, differing only in details: For instance, at the east coast of South America there is high MKE but low EKE. The high MKE is related to the northward flowing Malvinas Current, but since this current is attached to the continental slope with large bottom velocities it is stabilised by the bottom topography, leading to low EKE.

[9] Figure 1d shows an observational estimate of EKE in the Southern Ocean taken from satellite altimeter data (AVISO). Model simulation and observations agree well both in the location of high EKE regions and amplitudes of EKE in these regions. However, minimal values of EKE are lower in the model compared to observations. One reason for this discrepancy might be that the model underestimates EKE in quiescent regions such as the South Pacific north of 50°S , because of missing high-frequency wind stress forcing (the model is forced with monthly mean climatological forcing). On the other hand, the error level inherent to the altimeter data might inhibit smaller EKE levels.

[10] Figure 2a shows the Eulerian mean meridional stream function which is defined as

$$\frac{\partial}{\partial z} \psi_m(y, z) = \oint \bar{v}(x, y, z) dx \quad (1)$$

where v denotes meridional velocity, and \bar{v} the temporal average of v (over 5 years). At the northern boundary of the model domain, there is outflow of ca. 15 Sv of light water masses in the upper 1000 m, inflow of 34 Sv of NADW in the depth range of ca. 1000–3500 m and again outflow of ca. 12 Sv of AABW below 3500 m. Further to the south, however, there is a strong cell apparently transporting more than 30 Sv across (zonal and temporal mean) isopycnals. This is the well known Deacon Cell, with descent around $45\text{--}35^\circ \text{S}$ and ascent of water around $65\text{--}55^\circ \text{S}$ reaching depths of about 3000 m [Döös and Webb, 1994]. The Deacon cell is, similar to the Ferrell cells in the troposphere, an artifact of the zonal and temporal averaging of the flow [Karoly et al., 1997]. A physically more plausible interpretation of the meridional flow in the Southern Ocean is given by the residual stream function, shown in Figure 2b.

[11] The residual stream function, ψ , accounts for the effects of standing eddies (S) and transient eddies (T), i.e., $\psi = \psi_m + S + T$. Figures 2c and 2d show S and T with

$$S = \widehat{\rho^* v^*} L / \frac{\partial \hat{\rho}}{\partial z} \quad \text{and} \quad T = \widehat{\rho' v'} L / \frac{\partial \hat{\rho}}{\partial z} \quad (2)$$

where ρ denotes potential density, \hat{v} ($\hat{\rho}$, etc.) the zonal average of v (ρ , etc.), v^* (v') deviations from the zonal (temporal) average of v , and $L = L(y, z)$ the zonal length of the ocean. The resulting residual stream function ψ is similar to one in the eddy-permitting FRAM model [Döös and Webb, 1994] and POP model [Olbers and Ivchenko, 2001]. Note that ψ is much more aligned with the zonal mean isopycnals compared to ψ_m (Figure 2a).

3. Simulated Thickness Diffusivity

[12] The contributions T and S to the residual stream function ψ can be interpreted as a stream function, $\psi_{\text{eddy}} = T$

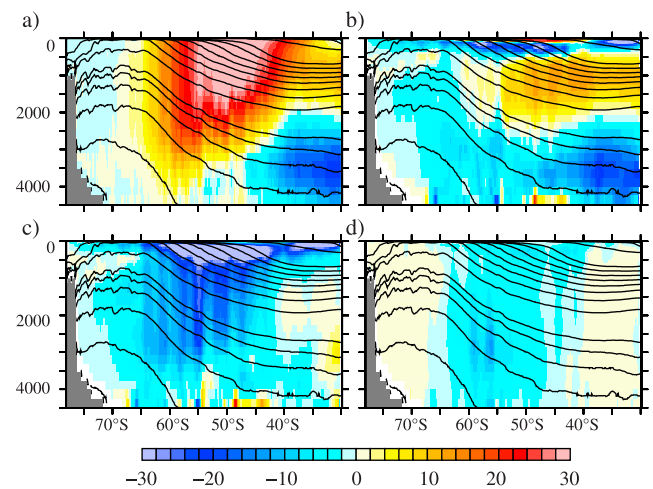


Figure 2. (a) Eulerian mean meridional stream function in Sv. (b) Residual stream function, see text for details. (c) Standing eddy contribution and (d) transient eddy contribution. Also shown are zonal mean isopycnals $\sigma_\theta = 26.5 \text{ kg/m}^3$, $\sigma_\theta = 27\text{--}27.8 \text{ kg/m}^3$ in 0.1 kg/m^3 and $\sigma_\theta = 27.8\text{--}28 \text{ kg/m}^3$ in 0.02 kg/m^3 spacing.

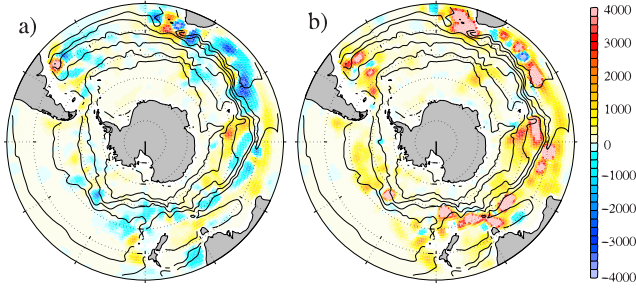


Figure 3. Thickness diffusivity, κ , at 300 m depth in m^2/s . (a) κ estimated from raw eddy fluxes (equation (4)) and (b) κ from equation (5), i.e., accounting for rotational fluxes, see text for details. Data are smoothed with a Hanning window over $5^\circ \times 5^\circ$. Also shown are mean buoyancy contours over $5^\circ \times 5^\circ$. $\sigma_\theta = 26.2, 26.4, 26.6, 26.8, 27.0, 27.2, 27.4, 27.6 \text{ kg/m}^3$.

+ S , for an eddy-driven meridional overturning. The three-dimensional analogue of such an eddy-driven meridional overturning is given by the bolus velocity \mathbf{u}^* [Gent et al., 1995] for which a (vector) stream function \mathbf{B} is given for the stratified interior of the ocean by

$$\mathbf{B} = \bar{\rho}_z^{-2} \begin{pmatrix} \bar{\rho}_z \bar{v}' \bar{\rho}' \\ -\bar{\rho}_z \bar{u}' \bar{\rho}' \\ \bar{\rho}_y \bar{u}' \bar{\rho}' - \bar{\rho}_x \bar{v}' \bar{\rho}' \end{pmatrix} \quad \text{with} \quad \mathbf{u}^* \equiv \nabla \times \mathbf{B} \quad (3)$$

The bolus velocity \mathbf{u}^* is added to the Eulerian mean velocity $\bar{\mathbf{u}}$ and the sum of both, i.e., the residual velocity, advects the mean tracer in e.g., a climate model. In the GM parameterisation, the fluxes $\bar{\mathbf{u}}'_h \bar{\rho}'$ in equation (3) are parameterised as

$$\mathbf{F}_h \equiv \bar{\mathbf{u}}'_h \bar{\rho}' = -\kappa \nabla_h \bar{\rho} - \nu (\mathbf{k} \times \nabla \bar{\rho})_h \quad (4)$$

with $\kappa = -|\nabla_h \bar{\rho}|^{-2} \mathbf{F}_h \cdot \nabla_h \bar{\rho}$ and $\nu = -|\nabla_h \bar{\rho}|^{-2} \mathbf{F}_h \cdot (\mathbf{k} \times \nabla \bar{\rho})_h$. The parameter κ denotes thickness diffusivity. The assumption that κ is positive ensures that the GM parameterisation releases available potential energy from the mean state [Gent et al., 1995]. The ν -component of the bolus velocity, on the other hand (which does not show up in the original GM parameterisation), can be interpreted in terms of a stream function for eddy-induced advection, rather than diffusion (which is related to κ) of mean isopycnal layer thickness, and shows up when horizontal mixing of buoyancy is anisotropic [Eden et al., 2006].

[13] Using $\bar{\mathbf{u}}'_h \bar{\rho}'$ from the eddy-resolving model, thickness diffusivity, κ , and its related parameter ν , can now be estimated. However, the estimation is thwarted by the presence of large rotational components in $\bar{\mathbf{u}}'_h \bar{\rho}'$ that have no effect on the mean buoyancy budget, but complicate the interpretation of the individual eddy tracer fluxes. Defining and removing different rotational fluxes leads to different diagnoses for κ and ν . Note that since the divergence of all possible flux decompositions is identical, the mean density budget for all flux decompositions is the same.

[14] Figure 3 shows the estimated κ in the Southern Ocean at 300 m depth. In Figure 3a no rotational flux was removed from $\bar{\mathbf{u}}'_h \bar{\rho}'$ prior to the analysis, resulting in

large regions with physically unphysical thickness diffusivities of negative sign. In Figure 3b the approach by Eden et al. [2006] was applied, i.e., κ and ν were estimated from

$$\kappa = -|\nabla_h \bar{\rho}|^{-2} (\mathbf{F}_h - \mathbf{k} \times \nabla \theta \cdot \nabla_h \bar{\rho}) \quad (5)$$

$$\nu = -|\nabla_h \bar{\rho}|^{-2} (\mathbf{F}_h - \mathbf{k} \times \nabla \theta) \cdot (\mathbf{k} \times \nabla \bar{\rho})_h \quad (6)$$

with $\theta = -|\nabla_h \bar{\rho}|^{-2} \overline{\mathbf{u}}_h \bar{\phi} \cdot (\mathbf{k} \times \nabla \bar{\rho})_h$ and where $\bar{\phi} = \frac{\bar{\rho}^2}{2}$ denotes density variance. In this setting, θ is given by the flux of variance along contours of mean density and it can be shown that under certain assumption [Eden et al., 2006] the rotational part of the horizontal eddy density flux circulates along contours of $\bar{\phi}$.

[15] Using equation (5), κ becomes positive throughout most of the Southern Ocean. This positive sign is in agreement with positive local production of EKE by release of mean available potential energy (i.e., related to $\bar{\rho}' w'$, not shown). In general, κ is large where EKE (and MKE) is large as well and κ tend to be larger at the poleward flank of the ACC with values exceeding $4000 \text{ m}^2/\text{s}$ in regions of high EKE.

[16] The parameter ν is shown in Figure 4, estimated according to equation (6). A band of negative ν extends from the southern tip of Africa through the Indian and Pacific into the Atlantic sector of the Southern Ocean, pointing toward eastward (westward) advection of isopycnal thickness at the poleward (equatorward) flank of the ACC. The regions of large amplitudes for ν coincide roughly with regions of high EKE and MKE. As illustrated by C. Eden (Towards a turbulence model for meso-scale eddies, submitted to Journal of Physical Oceanography, 2006, hereinafter referred to as Eden, submitted manuscript, 2006) anisotropic lateral mixing of density, indicated by large differences in the zonal and meridional characteristic eddy length scales, leads to an advective eddy-effect on isopycnal thickness. It appears that the ACC is a region with strong anisotropic lateral eddy mixing. Note, however, that both thickness diffusion (related to κ) and advection (ν) show up as advective effects in the density and tracer budget.

[17] To illustrate the depth dependency of κ , Figure 5 shows the zonally averaged κ ($\hat{\kappa}$) as estimated without removing any rotational fluxes (Figure 5a) and according

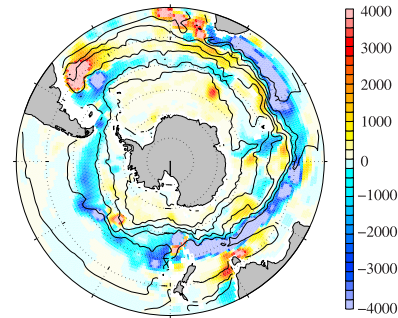


Figure 4. The stream function for isopycnal thickness advection, ν , at 300 m depth in m^2/s . Also shown are mean density contours (same as in Figure 3). Data are smoothed with a Hanning window over $5^\circ \times 5^\circ$.

to equation (5) (Figure 5b). Clearly $\hat{\kappa}$ decreases with depth, below ca. 2500 m the thickness diffusivity is essentially zero in both cases; a similar depth dependency can be seen for the parameter ν (not shown). Near the surface, however, κ in Figure 5b is much higher than κ estimated without removing a meaningful rotational flux (Figure 5a). It appears that much of the negative values of κ around a latitude (Figure 3a) cancel the positive values in a zonal average, while this is not the case for κ according to equation (5).

4. Summary

[18] Thickness diffusivities (κ) according to the GM parameterisation are estimated in an eddy-resolving model of the Southern Ocean using a physically meaningful definition of rotational eddy fluxes. Large horizontal and vertical variations are present in the estimated κ , which means that using a single constant value for κ in a non-eddy-resolving model is clearly inconsistent with these estimates. It was shown by *Ferreira et al.* [2005] and Eden (submitted manuscript, 2006) that such variations of κ have strong effects on the circulation and water mass characteristics in coarse resolution ocean models.

[19] In agreement with recent estimates from satellite data of near surface eddy diffusivities by *Marshall et al.* [2006], large (small) values of the thickness diffusivities show up equatorward (poleward) of the ACC. Figure 6 shows the near surface, zonally averaged κ , similar to Figure 4 of *Marshall et al.* [2006]. Poleward of 60°S, $\hat{\kappa}$ remains below 200 m²/s, between 60–45°S $\hat{\kappa}$ increases to about 600 m²/s and between 45–35°S $\hat{\kappa}$ peaks at almost 3000 m²/s. κ is high in regions with high EKE. Note that possible reasons for the structure in κ and implications for possible parameterisations are discussed by Eden (submitted manuscript, 2006).

[20] However, it should be noted that, in contrast to the suggestion by *Marshall et al.* [2006], in the mixed layer (Figure 6 and Figure 4 of *Marshall et al.* [2006]) the estimated κ corresponds to lateral, diapycnal diffusivity. Only well below the mixed layer κ becomes thickness diffusivity appropriate to the GM parameterisation. $\hat{\kappa}$ stays high in the upper 500 m but decreases with depth and is essentially zero below 2500 m.

[21] In addition to the thickness diffusivity κ , there is strong eddy-induced advection of isopycnal thickness (ν). There is eastward (westward) advection of isopycnal

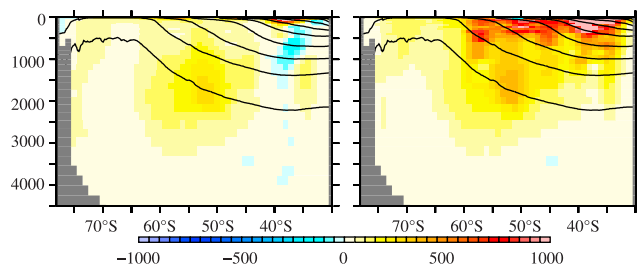


Figure 5. Zonally averaged κ estimated (a) from raw eddy fluxes and (b) according to equation (5) in m²/s. Also shown are zonal mean isopycnals $\sigma_\theta = 26\text{--}28\text{ kg/m}^3$ in 0.25 kg/m^3 spacing.

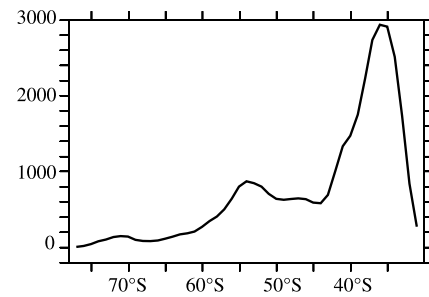


Figure 6. Zonally averaged κ at 50m depth in m²/s according to equation (5).

thickness at the poleward (equatorward) flank of the ACC pointing toward strong anisotropic lateral mixing.

[22] **Acknowledgments.** The author benefitted from discussions with Richard Greatbatch and Heiner Dietze. The model integrations have been performed on a NEX-SX8 at the University Kiel and on a NEC-SX6 at the Deutsches Klimarechenzentrum (DKRZ), Hamburg.

References

- Bryan, K., J. K. Dukowicz, and R. D. Smith (1999), On the mixing coefficient in the parameterization of bolus velocity, *J. Phys. Oceanogr.*, 29, 2442–2456.
- Döös, K., and D. J. Webb (1994), The Deacon cell and the other meridional cells of the Southern Ocean, *J. Phys. Oceanogr.*, 24(2), 429–442.
- Eden, C., R. J. Greatbatch, and J. Willebrand (2006), A diagnosis of thickness fluxes in an eddy-resolving model, *J. Phys. Oceanogr.*, in press.
- England, M. H., and S. Rahmstorf (1998), Sensitivity of ventilation rates and radiocarbon uptake to subgrid-scale mixing in ocean models, *J. Phys. Oceanogr.*, 29, 2802–2827.
- Ferreira, D., J. Marshall, and P. Heimbach (2005), Estimating eddy stresses by fitting dynamics to observations using a residual-mean ocean circulation model and its adjoint, *J. Phys. Oceanogr.*, 35, 1891–1910.
- Gent, P. R., and J. C. McWilliams (1990), Isopycnal mixing in ocean circulation models, *J. Phys. Oceanogr.*, 20, 150–155.
- Gent, P. R., J. Willebrand, T. J. McDougall, and J. C. McWilliams (1995), Parameterizing eddy-induced tracer transports in ocean circulation models, *J. Phys. Oceanogr.*, 25, 463–474.
- Karoly, D., P. C. McIntosh, P. Berrisford, T. J. McDougall, and A. C. Hirst (1997), Similarities of the Deacon cell in the Southern Ocean and Ferrel cells in the atmosphere, *Q.J.R. Meteorol. Soc.*, 123(538), 519–526.
- Marshall, J., and G. Shutts (1981), A note on rotational and divergent eddy fluxes, *J. Phys. Oceanogr.*, 11(12), 1677–1679.
- Marshall, J., E. Shuckburgh, H. Jones, and C. Hill (2006), Estimates and implications of surface eddy diffusivity in the Southern Ocean derived from tracer transport, *J. Phys. Oceanogr.*, in press.
- Medvedev, A. S., and R. J. Greatbatch (2004), On advection and diffusion in the mesosphere and lower thermosphere: The role of rotational fluxes, *J. Geophys. Res.*, 109, D07104, doi:10.1029/2003JD003931.
- Olbers, D., and V. O. Ivchenko (2001), On the meridional circulation and balance of momentum in the Southern Ocean of POP, *Ocean Dyn.*, 52, 79–93.
- Pacanowski, R. C. (1995), MOM 2 documentation, user's guide and reference manual, *Tech. Rep. 3*, Ocean Group, Geophys. Fluid Dyn. Lab., Princeton, N. J.
- Phillips, H. E., and S. R. Rintoul (2000), Eddy variability and energetics from direct current measurements in the Antarctic Circumpolar Current south of Australia, *J. Phys. Oceanogr.*, 30, 3050–3076.
- Rintoul, S. R., C. Hughes, and D. Olbers (2001), The Antarctic Circumpolar Current system, in *Ocean Circulation and Climate*, pp. 271–302, Elsevier, New York.
- Rix, N., and J. Willebrand (1996), A note on the parameterisation of eddy-induced mixing from eddy-resolving model data, *J. Phys. Oceanogr.*, 26, 2281–2285.

C. Eden, FB I, Ocean Circulation and Climate Dynamics, IFM-GEOMAR, Düsternbrooker Weg 20, D-24105 Kiel, Germany. (ceden@ifm-geomar.de)